Journal of Applied Polymer Science

Chitosan-based gel film electrolytes containing ionic liquid and lithium salt for energy storage applications

Jeremy Chupp,[1] Annadanesh Shellikeri,[2] Goutam Palui,[3] Jhunu Chatterjee[1]

[1]High Performance Materials Institute, Florida State University, Tallahassee, Florida 32310

[2]Aeropropulsion, Mechatronics and Energy Centre, Department of Electrical Engineering, FAMU-FSU College of Engineering, Tallahassee Florida 32310

[3]Department of Chemistry, Florida State University, Tallahassee, Florida 32308

Correspondence to: J. Chatterjee (E-mail: jhunu@eng.fsu.edu)

ABSTRACT: Fabrication, characterization, and a comparative study have been performed for chitosan-based polymer electrolytes using two different dispersion media. Chitosan gel film (solid) electrolytes are fabricated using acetic acid or adipic acid as the dispersant for chitosan in combination with ionic liquid and lithium salt. This quaternary system of chitosan, acetic acid or adipic acid, 1-butyl-3-methylimadazolium tetrafluoroborate (ionic liquid), and lithium chloride is formed as an electrolyte for potential secondary energy storage applications. The ionic conductivities, thermal, structural, and morphological properties for these electrolytes are compared. The ionic conductivities for chitosan/adipic acid (CHAD) and for chitosan/acetic acid (CHAC) systems are in the range of $3.71 \times 10^{-4}-4.6 \times 10^{-3}$ and $1.3 \times 10^{-4} -3.2 \times 10^{-3}$ S cm^{-1}, respectively. The thermal stability of CHAD-based electrolytes is determined to be higher than that of CHAC-based electrolytes. Preliminary studies are performed to determine the electrochemical stability of these materials as solid film electrolytes for electrochemical supercapacitors. © 2015 Wiley Periodicals, Inc. J. Appl. Polym. Sci. **2015**, *132*, 42143.

KEYWORDS: batteries and fuel cells; biodegradable; biopolymers and renewable polymers; electrochemistry; properties and characterization

Received 14 November 2014; accepted 23 February 2015

DOI: 10.1002/app.42143

INTRODUCTION

Electrochemical energy storage systems (e.g., batteries and supercapacitors) play a vital role in applications, such as portable electronics, medical equipment, electric vehicles, military devices, and the storage of energy from renewable sources.[1] The advancements in these technologies increase the demand for electrochemical energy storage systems to achieve higher levels of performance[2] in terms of the energy density, power density, life cycle, cost, temperature range, stability, safety, impact to the environment, and flexibility to meet various design needs.[3,4]

Currently used electrochemical storage systems, such as primary cells, secondary cells, and fuel cells, suffer from serious problems, such as leakage, toxicity, and high cost of proper disposal, resulting in unsuitable long-term opportunities.[1] A large amount of research is being performed to create and modify various components in energy storage systems to minimize these factors. This study focused on creating a natural polymer-based solid electrolyte to address the issues above because electrolytes play a very important role in any electrochemical energy storage system. Numerous solid polymer gel-based electrolytes using polyvinyl alcohol (PVA), polyethylene oxide (PEO), polyvinylidene fluoride (PVDF), polyacrylonitrile (PAN), and polymethyl methacrylate (PMMA)[5–10] have been reported and are being used based on cross-linked polymer network structures with an organic liquid (e.g., ethylene carbonate, propylene carbonate, diethyl carbonate, etc.) and lithium-based[5] salts. However, they suffer from issues such as volatility, thermal instability, and flammability.

Here we report the fabrication procedure for natural polymer and ionic liquid-based solid electrolyte systems and compare

This article was published online on 16 March 2015. An error was subsequently identified. This notice is included in the online and print versions to indicate that both have been corrected 28 March 2015.

Additional Supporting Information may be found in the online version of this article.

their properties in terms of the ionic conductivity, thermal stability,[4] structure, and morphology. Natural biopolymers, such as chitosan and cellulose, are low-cost alternatives to the synthetic polymers mentioned.[1] Chitosan is nontoxic, biodegradable, and abundant in nature. The polysaccharide copolymer structure of chitosan is composed of linked D-glucosamine units with N-acetyl glucosamine units. Therefore, it is easily cross-linked with bi-functional compounds containing amine and/or hydroxyl groups.[11] Acetic acid has been commonly used for the dissolution of chitosan.[2] In this article, adipic acid has also been used to dissolve chitosan. The chemical and physical properties of the cross-linked chitosan depend upon the conditions under which they are obtained, specially on the structure of the cross linker. Thus, the system with adipic acid is different than the system with acetic acid because of the dissolution and cross-linking effects of adipic acid with chitosan. It has been reported that adipic acid enhances the thermal stability of natural polymers,[12] and this study also shows that the chitosan/adipic acid system has greater thermal stability than the chitosan/acetic acid system. The solid electrolyte systems described here have used a room-temperature ionic liquid (RTIL), mainly for enhanced ionic conductivity and for film processability. Recently, ionic liquids (ILs) have attracted interest for use as an electrolyte because of their unique properties, such as their high thermal stability, large liquid-phase temperature range, electrochemical stability, excellent ionic conductivity,[2,4,13] and plasticizing and lubricating properties.[14–16] ILs can be recycled, which is environmentally friendly and has the potential to lower the cost of the synthesis process. In the first step, a gel electrolyte consisting of the host polymer chitosan was synthesized using acetic acid or adipic acid, separately, along with a lithium salt (lithium chloride, LiCl) to increase the conductivity and to enable use in lithium ion batteries or in electrochemical capacitors. Another reason for using lithium salt is that it has excellent solubility in polymers, such as polyvinyl alcohol and it does not crystallize during the drying process of gel.[17] Thermal and impedance data were obtained to determine the effect of the dispersing medium as well as the effect of the concentration of the salt on the thermal stability and ionic conductivity of the gel film samples. Scanning electron microscopy was performed to study the morphological characteristics of the gel film samples. Structural (chemical) analysis for gel samples was performed using FTIR. The electrochemical stability and cyclability for this electrolyte system were studied to explore the possibilities of using these systems in electrochemical capacitors.

EXPERIMENTAL

Preparation of CHAC/IL/LiCl or CHAD/IL/LiCl Gel Film Electrolyte

Glacial acetic acid (AC, EMD, GR ACS) was diluted to a 1% solution with DI water. Chitosan (CH, Sigma-Aldrich, Medium molecular weight, 190KD-310KD) was added to 10 mL of a 1% acetic acid solution to produce a 2% (w/v) solution of chitosan acetate. This solution was stirred at room temperature for 2 hours. Following the complete dissolution of CH, lithium chloride (LiCl, Alfa Aesar, ACS 99% min.) was added in various concentrations of 0–50% (w/w) based on CH, and stirring was continued for 1 hour. The solution was cast onto a glass slide and immersed in a 10% (w/v) sodium hydroxide (NaOH, Sigma-Aldrich, 97% ACS reagent) aqueous solution for 20 minutes. The samples were rinsed with DI water several times to remove excess NaOH before soaking in an excess of ethanol (Et, Sigma Aldrich, >99.5% reagent grade) for 24 hours. Finally, the samples were soaked in 2 mL of 1-butyl-3-methylimidazolium tetrafluoroborate ($BMImBF_4$, Sigma-Aldrich) for 10 minutes. The gel film containing acetic acid (CHAC) was dried at 70°C for 48 hours. A 1% (w/v) adipic acid (AD, Sigma Aldrich) solution was substituted for acetic acid following the procedure mentioned above to produce the gel films with adipic acid (CHAD). The films had a thickness of approximately 0.1 mm. The electrolyte films were named with the corresponding salt concentration of each sample preceded by the sample name CHAC or CHAD (e.g., the chitosan/acetic acid film containing 10% salt was named CHAC_10). The sample names ended with NIL means that those samples have no ionic liquid (NIL). Six different compositions for each system (acetic and adipic) were made, varying the salt concentration from 5% to 50% with respect to the amount of chitosan.

Characterization

Ionic Conductivity. The gel film samples were placed in a teflon tube and sandwitched between two pieces of 2-in nickel rods. The nickel rods placed at both ends are pressed tightly against the gel film sample in order to avoid any air gap. These nickel rods were acted as blocking electrodes and the whole assemblies were made in a glove box. The whole assembly was then connected to a Versastat 3 potentiostat (Princeton Analytical Instruments). The ionic conductivity of the gel electrolytes was measured by using AC impedance spectroscopy with AC signal amplitude of 20 mV. The AC impedance spectra were acquired from 10 Hz to 100 kHz for all of the samples. The highest frequency impedance value gives the bulk resistance of the gel electrolytes, R_b, from which the ionic conductivity, σ, of the gel electrolyte was determined using the relation

$$\sigma = \frac{L}{AR_b} \tag{1}$$

where L is the distance between the two Ni-rod (Dia = 12.75 mm) current collectors, and A is the cross-sectional area of the Ni rod. All measurements were performed at room temperature.

Temperature-Dependent Ionic Conductivity. The ionic conductivity was also determined in a temperature range of 25–100°C to study the temperature dependence of ionic conductivity and the thermal stability of these electrolyte systems.

Thermal Properties. All of the dry film samples were subjected to thermal analysis using a TA Q50 thermogravimetric analyzer (TA instruments) in the presence of nitrogen (40−900°C at a scan rate of 20°C min^{-1}).

Structural and Morphological Property. A Thermo Nicolet 6700 Fourier Transform Infrared (FT-IR) Spectrometer with a golden gate attachment was used for obtaining FTIR spectra for all gel film electrolytes. For the ionic liquid, a pellet with potassium bromide (KBr) was made as follows: 1 mg of ionic liquid was mixed with 99 mg of KBr. The mixture was ground until the IL was evenly distributed throughout the KBr, without any

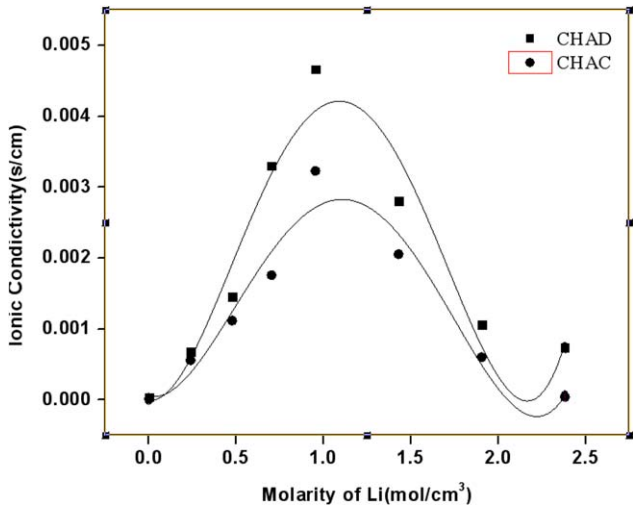

Figure 1. Variation in the ionic conductivity with the lithium salt concentration (the concentration of the IL remained the same in all samples). [Color figure can be viewed in the online issue, which is available at wileyonlinelibrary.com.]

noticeable aggregates. The ground KBr powder mixed with IL were placed under three metric tons of pressure for 5 s. The pellet was retrieved and loaded into the FT-IR to obtain the spectra.

A JEOL SEM (JSM 7401FE) was used to observe the freeze-fractured surface of the gel film samples. The film samples were freeze-fractured in liquid nitrogen and mounted onto a regular 26-mm aluminum stub. The samples were then sputter-coated with gold and observed in the SEM at an accelerating voltage of 10 kV. An optical microscope (Olympus BX40) was used to observe the surface of gel film electrolytes.

Electrochemical Stability and Cyclability. Although high ionic conductivity is a desirable property for an electrolyte, cyclability and electrochemical stability are very important parameters for its use in a solid-state electrochemical capacitor. A CHAC_20 sample of 0.1 mm thickness was used to make a EDLC using carbon nanotube (CNT) bucky paper (BP) (obtained from Nanocomp) as the electrode, and cyclic voltammetry was run at various scan rates to determine the electrochemical stability of this solid electrolyte. Typical galvanic charge/discharge cycling was also performed using a 50-mA current.

RESULTS AND DISCUSSION

Ionic Conductivity

In Figure 1, the ionic conductivity reaches a maximum at approximately 20% salt concentration for the same amount of polymer in all gel film samples. The lithium salt molarity was calculated with respect to the chitosan (weight) and the total volume of chitosan and ionic liquid. Because the amount of acid, sodium hydroxide, and ionic liquid were held constant in all samples (CHAC and CHAD), the increase in the ionic conductivity is only because of the increase in the salt concentration, or in other words, is because of the increased number of charged carriers (Li^+ and Cl^-). As shown in Figure 1, at a higher Li salt concentration ($> 0.9M$) the ionic conductivity value decreases. The increased amount of salt increases the viscosity, and the formation of ion pairs and cluster formation resulted in a reduction in the ionic conductivity. At highest lithium concentration (2.38 moles/L), the ionic conductivity value for CHAD series dropped to 7.40×10^{-5} s/cm from 4.66×10^{-3} s/cm (at 0.95 moles/L) and for CHAC series ionic conductivity value dropped to 4.08×10^{-5} s/cm (LiCl, 2.38 moles/L) from 3.23×10^{-3} s/cm (0.95 moles/L). Because of the presence of the ionic liquid, the reduction in the ionic conductivity is not significant compared to the behavior of many other systems in which an increase in salt concentration beyond an optimum value results in a significant reduction in the ionic conductivity [5,18,19].

Role of Ionic Liquid in Film Processability

In this chitosan film electrolyte, the ionic liquid acted as a plasticizer, and because of its compatibility with the chitosan film, the IL is able to permeate into the free volume around the cross-linked polymer chains. This interaction had several consequences. First, it imparted ionic conductivity to the polymer films. Second, it increased the intermolecular distance, which results in swelling and an increased free volume. Finally, as a result of the increased free volume and decreased secondary bonding forces, the IL acts as a lubricant[14–16] that enhances the chain mobility, and the polymer molecules move easily in response to an applied load. It is difficult to peel the films without IL off the glass slide, whereas the films with IL can easily be peeled off. (Supporting Information Figure S1).

Structural and Morphological Analysis

FTIR studies were conducted on the film samples, and Figure 2(a,b) represent the combined spectra for the CHAC and CHAD systems, separately, and Figure 2(c) represents the spectra for the IL. The spectral details suggest the presence of NH_3^+ and COO^- in both figures (1665−1670, 1560−1570, 1530−1535, and 1450–1470 cm^{-1}). It is clear from the data that, as a result of self-assembly, the characteristic features of the NH and CH stretching and NH bending become more prominent in all gel film samples rather than the broad one present in the powder form, especially in the CHAC series. Almost insignificant signal because of –NH bonds (−1650 cm^{-1}) for CHAC_20, compared to pure chitosan, indicates the complex formation through the interaction of the lithium cations derived from the salts (∼20%) with the lone pair of electrons on the nitrogen atom present in the amino group of chitosan.[20] In addition to this, in the case of CHAD_20, the shift in the amide band and the NH_3^+ band toward lower wavenumber is observed, which confirms the cross-linking of the chitosan molecules through the carboxylate head groups. Thus, in other words, it can be concluded that adipic acid provides more cross-linking than acetic acid and thus more robustness to the film. However, it is difficult to conclude the type of interaction between the ionic liquid and the rest of the components in these ternary systems, other than the electrostatic interaction. In Figure 2(b), CHAD_0 and CHAD_20 exhibited peaks from the presence of the IL (as observed in the FTIR of the IL in Figure 2(c) and at 2960 and 3150 cm^{-1}. The CHAC samples showed no significant peaks because of the presence of the IL. For both the CHAC and CHAD systems, other than a weaker

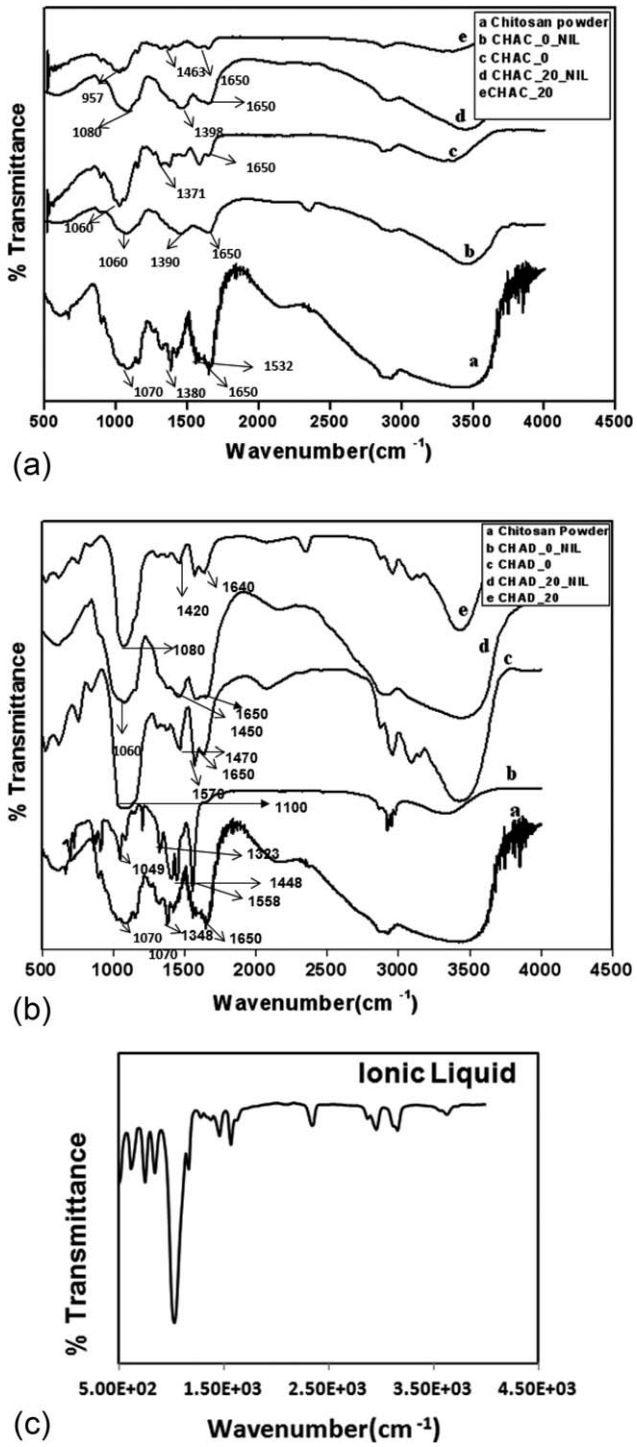

Figure 2. (a) FTIR spectra for the CHAC system. (b) FTIR spectra for the CHAD system. (c) FTIR spectra for the Ionic liquid.

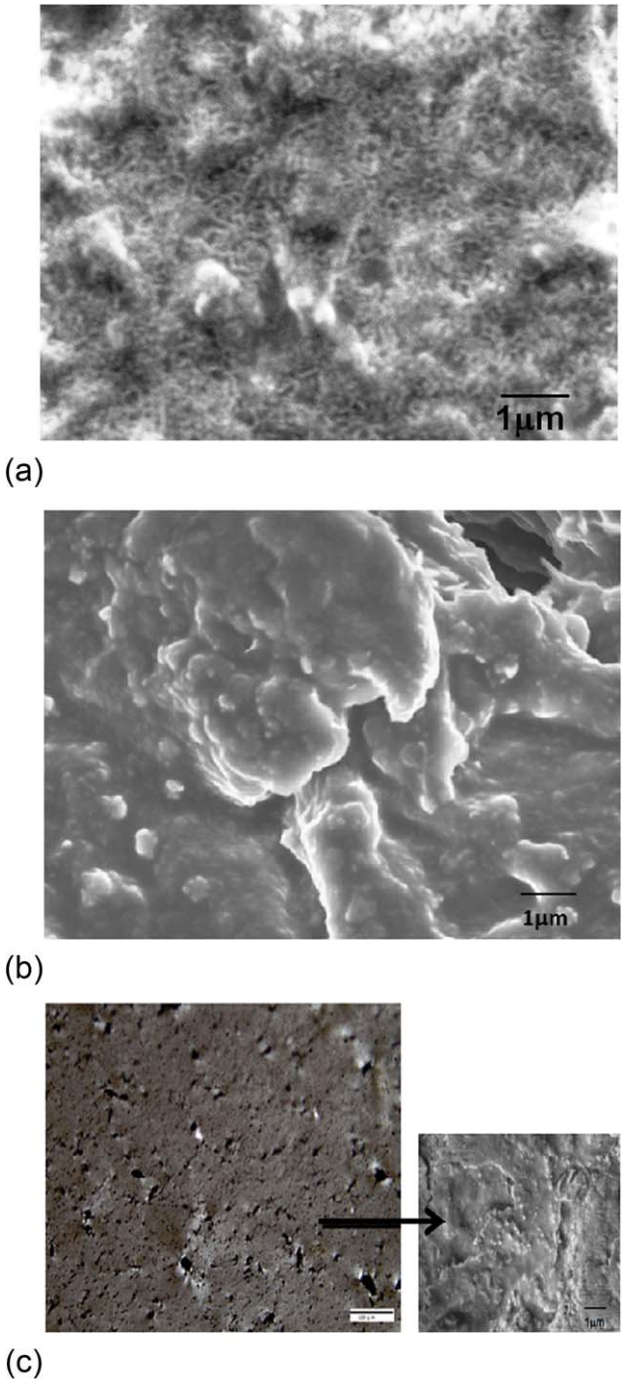

Figure 3. (a) SEM images for the CHAC gel system without a lithium salt or ionic liquid. (b) Combined optical and SEM images for the CHAC_20 gel film samples. (c) SEM images for the CHAD_20 gel film samples. [Color figure can be viewed in the online issue, which is available at wileyonlinelibrary.com.]

signal in the region of 1200−1400 cm^{-1} than for pure chitosan, no major change was observed because of the presence of the IL. Thus, it is difficult to detect a role of IL in the form of chemical bonding with other components, other than its role as a plasticizer during film formation.

Figures 3(a–c) are SEM micrographs of CHAC_0 _NIL, CHAC_ 20 and CHAD_ 20, respectively. Figure 3(a) is a gel film of chitosan and acetic acid without any salt or ionic liquid in it. It has greater porosity than the cross-linked film electrolytes CHAC_20 and CHAD_20. Figure 3(b) is a combination of an optical image and a scanning electron micrograph. The larger part of this figure is an optical micrograph of the surface of CHAC_20, and the

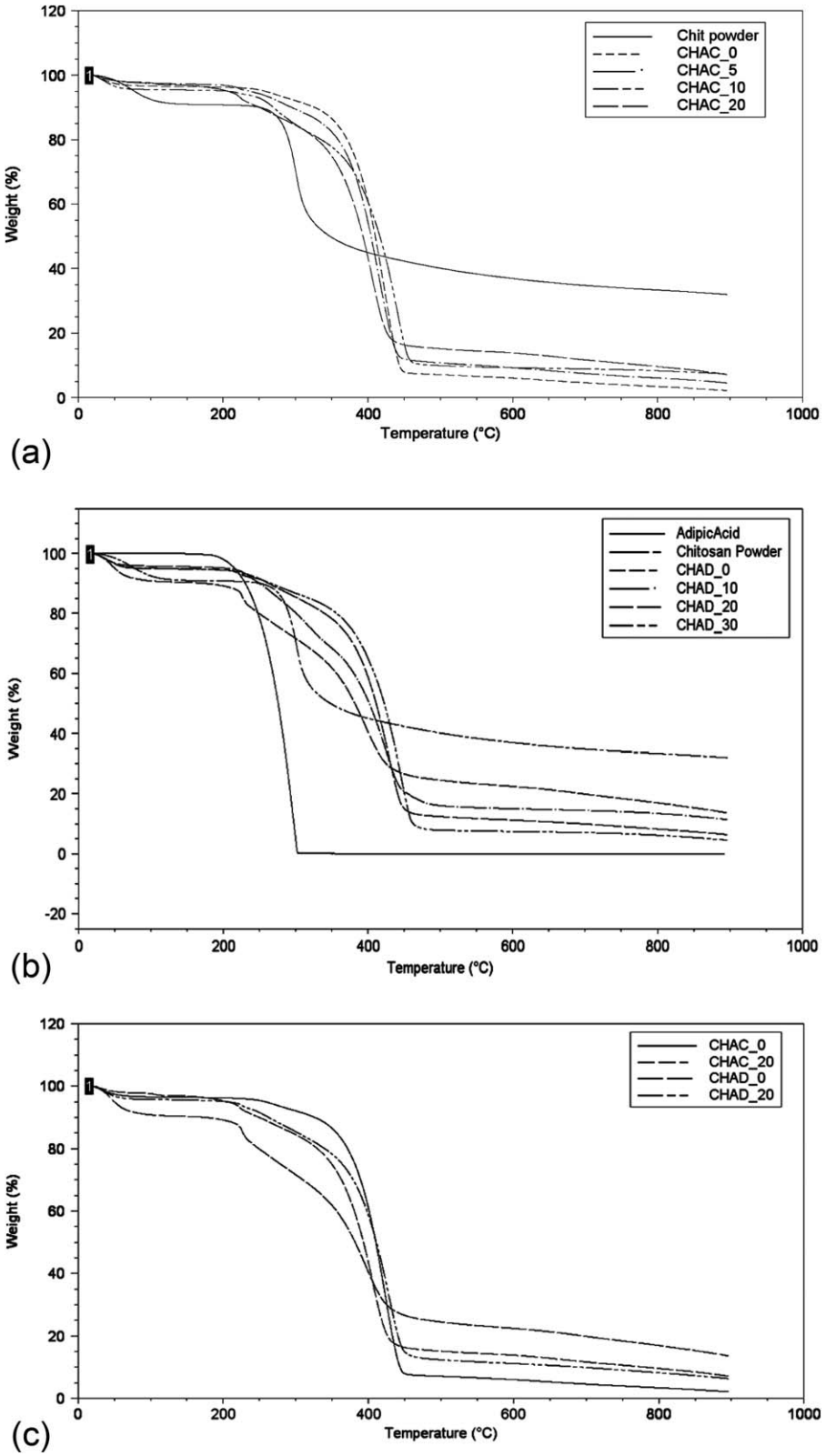

Figure 4. (a) Thermogravimetric analysis plot for the CHAC system. (b) Thermogravimetric analysis plot for the CHAD system. (c) Thermogravimetric analysis combined plot for the CHAC-CHAD system.

smaller image is the scanning electron micrograph for the same sample with higher magnification. Porous structure of film was observed which is very similar as typical gel sample. The typical pore sizes are in the range of 1−10 μm. In both cases [3(b) and 3(c)], a globular structure was observed for the polymer.

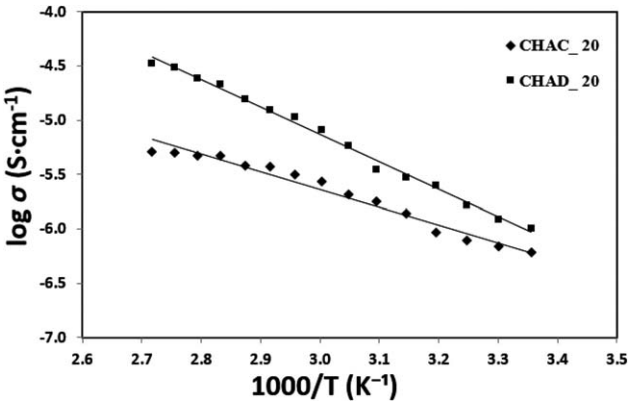

Figure 5. Variation in the ionic conductivity with temperature for various gel electrolyte films.

Thermogravimetric Analysis

Figures 4(a,b) represent the thermogravimetric analysis plots for the CHAC and CHAD systems. For the chitosan/acetic acid system, there is a decrease in the degradation with increased salt concentration, whereas, in case of the CHAD system, the degradation temperature increased with increasing salt concentration. In both, the system decomposition starts at a higher temperature than for pure chitosan. The incorporation of both acetic acid and adipic acid played a role to increase the thermal stability, as observed from the shift in the decomposition temperature. Because of its additional cross-linking with chitosan through both carboxylic acid groups, adipic acid showed enhanced thermal stability with increasing salt concentration.[21] Further, experimental results showing the temperature dependence of the conductivity also support these results. Figure 4(c) shows a combined plot for two different concentrations of CHAC and CHAD systems, and the CHAD system exhibited a higher degradation temperature than the CHAC system.

Temperature Dependence of the Conductivity

Figure 5 shows the temperature dependence of the conductivity for the CHAC and CHAD systems. Because the compositions of both CHAC_20 and CHAD_20 showed higher conductivity than that of the other compositions, these two samples were selected for graphical representation of their conductivities measured in the temperature range of 30−100°C. The plots of these data show a linear relationship that confirms that the variation in the ionic conductivity with temperature obeys the characteristics of an Arrhenius-type thermally activated process.[1] From the plot of log σ vs. 1000/T, the activation energy was calculated based on Arrhenius equation

$$\sigma = \sigma_0 \exp\ (-\mathrm{Ea}\ /kT)$$

where σ_0 is pre-exponential factor, Ea is the activation energy, T is the absolute temperature, and k is Bolzman's constant. As shown in Table I, activation energy values for three different compositions in both series of samples decreases with increase in ionic conductivity. (The Ea values were calculated based on the slope obtained by using the Supporting Information data in Tables S1 and S2) .The increase of conductivity with temperature is interpreted as a hopping mechanism between coordinating sites, local structural relaxation and segmental motion of the polymer salt complexes.[22,23] With the increase of temperature the polymer chains have faster internal bond rotations, producing segmental motion and hence favoring interchain and intrachain ion movements, thus increase of conductivity appears.[24]The conductivity of the film samples ranged from approximately 10^{-3} to 10^{-2} S cm^{-1} between 30°C and 100°C. The difference in the ionic conductivities between CHAD film samples with CHAC film samples increased at higher temperature, which can most likely be explained by the retention of a higher salt concentration in the more cross-linked structure of adipic acid with the chitosan complex than for the acetic acid-chitosan samples. Supporting Information data (in Tables S1 and S2) can be used to support this observation.

Table I. Activation Energy for Different CHAC and CHAD Samples at 30°C

Sample (with different Li Cl content, wt %)	σ (S·cm^{-1})	Ea (ev)	Std. Dev.
CHAC_10	2.00E-03	0.221	0.012
CHAC_20	2.11E-03	0.140	0.003
CHAC_30	2.91E-03	0.200	0.002
CHAD_10	1.08E-03	0.269	0.004
CHAD_20	2.71E-03	0.218	0.008
CHAD_30	2.67E-03	0.221	0.001

Electrochemical Stability and Cyclability

The newly developed gel film electrolyte (CHAC_20) was analyzed for its stability and lithium-ion conduction for its application as a solid electrolyte and separator in an all solid state energy storage device. Cyclic voltammetry was performed (scan rates ranging from 5 to 400 mV/s) on a symmetric capacitor with a two electrode configuration of BP||GEL film Electrolyte (separator) ||BP, assembled for this purpose. As seen in Figure 6(a), the system appears to be stable over a broad range of −2 to 2 V (electrochemical potential window of 4 V). Even at a high scan rate of 400 mV/s, the system gives a stable mirror image symmetric response about the x-axis, pointing towards the optimum operation of the gel separator as a lithium-ion conducting electrolyte promoting the formation of double layer at the electrolyte-electrode interfaces. For industrial application of the Gel film electrolyte, the long-term stability during cycling is a major demand.[25] Hence, the cycle life study coulombic efficiency was estimated for the assembled solid state capacitor. The galvanic charge/discharge cycles were performed at a 50 μA constant current. The continuous cycling was performed and it exhibits typical triangular charge/discharge profiles[26,27] over subsequent cycles, with a negligible potential drop. Further, there is very little sag or slump is the discharge curve, which can be correlated to the suppressed pseudocapacitive peaks in the CV curves shown in Figure 6(a). Their triangular profiles and low potential drops indicate towards a very high coulombic efficiency over multiple cycles.[28] This is verified in Figure 6(b), where a high coulombic efficiency of 94% is maintained even after 1500 cycles and the minimal change in cycle profile between the 1st and the 1500th cycle, shown in Figure 6(b),

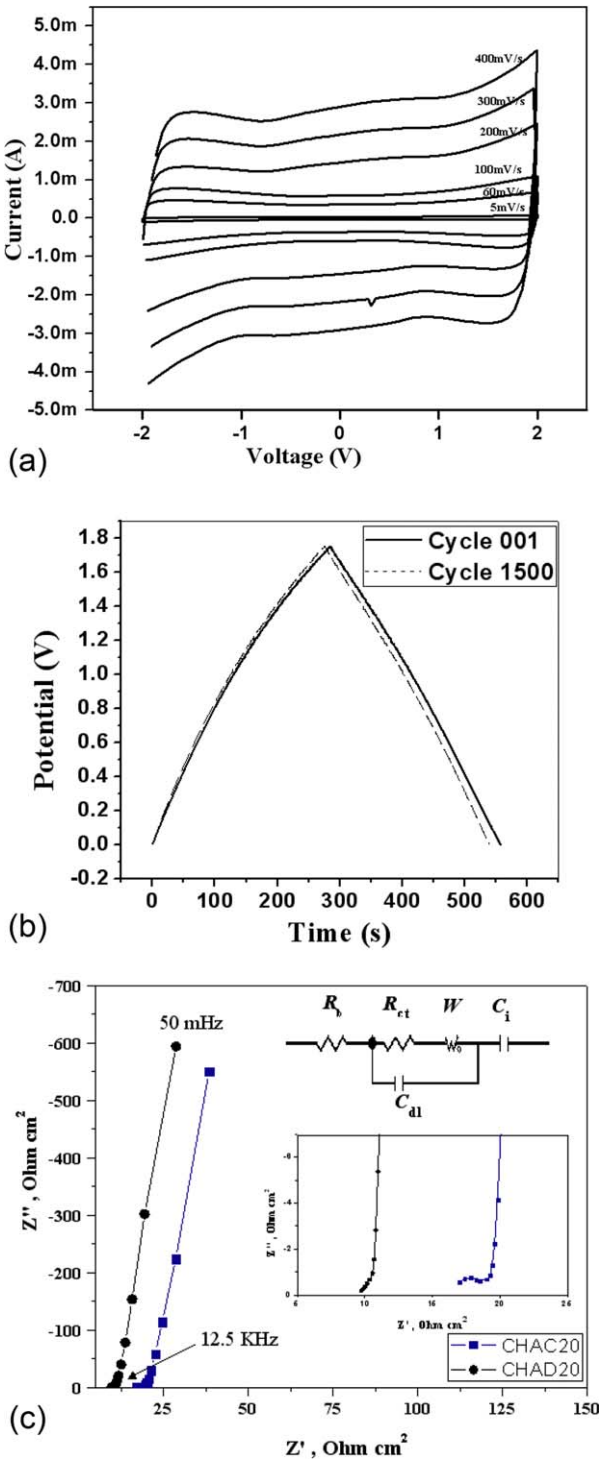

Figure 6. (a) Cyclic voltametry plots for the CHAC_20 system at various scan rates. (b) Charge/discharge curve of the BP||GEL film electrolyte (CHAD_20)||BP cell assembly at a constant current of 50 μA. (c) Electrochemical impedance profiles for the gel film electrolyte systems. [Color figure can be viewed in the online issue, which is available at wileyonlinelibrary.com.]

points towards a good cycle life, again indicating towards a stable operation of the system using the solid state electrolyte and the ability of the device to operate as a power source. Further analysis of the electrochemical properties of the CHAC_20 and CHAD_20 gel film electrolytes was performed by analysis of the impedance spectra of the assembled solid state capacitors using these electrolytes. Figure 6(c) shows the complex impedance plot (Nyquist plot) of the symmetric capacitor with a BP||GEL film Electrolyte (separator) ||BP configuration. A good capacitor-like behavior is indicated by a steeply rising imaginary part (Z'') in the low-frequency region[29] for both CHAD_20 and CHAC_20 samples, which reveals the adsorption quality of the ions on the electrolyte-electrode interface. The mid to high-frequency region are contributed by the ion-diffusion transport, charge transfer or interfacial interactions, and bulk material properties. To investigate these regions, an expanded part of the recorded EIS spectra are presented as an inset in Figure 6(c). Clearly there is a marked difference between the two samples in this mid frequency region, with CHAC_20 showing a larger diffusion limitation through its larger, more prominent semicircle. The bulk resistances, determined from the *x*-axis intercepts of the EIS spectra in the low-frequency region, for capacitors assembled using CHAC_20 and CHAD_20 film electrolytes/separators were observed to be 16.6 and 9.5 Ω cm^2 respectively. Lower internal resistance of the CHAD_20 capacitor is partly contributed by the higher ionic conductivity exhibited by CHAD_20 compared to CHAC_20, resulting in better ionic mobility and transport. An equivalent circuit is shown as an inset in Figure 6(c), which was used to fit the Nyquist plots of the CHAC_20 and CHAD_20 samples. The bulk properties of the two IL-based polymer electrolytes CHAC_20 and CHAD_20, are represented by the bulk resistance (R_b) appearing in the low-frequency region,[30] while the charge transfer resistance (R_{ct}) which appears in the mid to low-frequency region represents the bulk resistances at the electrolyte-electrode interfaces which the charge carriers have to overcome during interfacial transport. The mid frequency semicircle seen in CHAC_20 represents a combination of this charge transfer resistance and double layer capacitance (C_{dl}). The capacitive behavior observed through the high-frequency region steeply rising imaginary part is represented by the double layer formation at the interfaces (C_i), while the 45° slope region observed prominently for CHAD_20 and less prominently for CHAC_20 in the mid frequency region is represented by the Warburg impedance element (W).[26, 31] As expected, a high R_{ct} value of 0.3 Ω cm^2 was observed for CHAC_20 because of its lower conductivity values compared to CHAD_20 for which it was 0.12 Ω cm^2.

CONCLUSIONS

Solid, anhydrous polymer-film electrolytes comprising chitosan, adipic/acetic acid, an ionic liquid and a lithium salt have been fabricated with ionic conductivities in the order of 10^{-3} s cm^{-1}. It was observed in both systems that the ionic conductivity and processability of a complex system can be enhanced by an ionic liquid. Adipic acid can act as an equally efficient dispersing agent for chitosan as the conventional acetic acid, and it additionally can act as a cross-linking agent for a chitosan-based gel system. The use of a chitosan film complexed with an IL has been reported as an electrolyte and separator for an electrochemical supercapacitor. In our work, we have demonstrated

the electrochemical stability of these solid electrolytes over a broad range. Additionally, the presence of a lithium salt with the IL in the chitosan matrix opens up the possibility of using this type of solid electrolyte for lithium-battery applications.

ACKNOWLEDGMENTS

The authors gratefully acknowledge the necessary funding provided by the Department of Industrial and Manufacturing Engineering to support this research. The authors also would like to acknowledge the instrument facilities provided by the High Performance Materials Institute, Department of Chemistry and Department of Electrical Engineering at Florida State University

REFERENCES

1. Idris, N. K.; Nik Aziz, N. A.; Zambri, M. S. M.; Zakaria, N. A.; Isa, M. I. N. *Ionics* **2009**, *15*, 643.
2. Yamagata, M.; Soeda, K.; Ikebe, S.; Yamazaki, S.; Ishikawa, M. *Electrochim. Acta* **2013**, *100*, 275.
3. Daniel, C.; Besenhard, J. O., Eds. Handbook of Battery Materials, 2nd ed.; Wiley-VCH Verlag: Weinheim, **2011**.
4. Pandey, G. P.; Kumar, Y.; Hashm, S. A. *Ind. J. Chem.* **2012**, *49*, 743.
5. Chatterjee, J.; Liu, T.; Wang, B.; Zhang, J. P. *Solid State Ion.* **2010**, *181*, 531.
6. Agrawal, S. L.; Awadhia, A. *Bull. Mater. Sci.* **2010**, *27*, 523.
7. Song, J. Y.; Wang, Y. Y.; Wan, C. C. *J. Power Sources* **1999**, *77*, 183.
8. Li, G.; Li, Z.; Zhang, P.; Zhang, H.; Wu, Y. *Pure Appl. Chem.* **2008**, *80*, 2553.
9. Lee, K.; Park, J.; Kim, W. *Electrochim. Acta* **2000**, *45*, 1301.
10. Osman, Z.; Ansor, N. M.; Chew, K. W.; Kamarulzaman, N. *Ionics* **2005**, *11*, 431.
11. Fang, Y.; Hu, D. *Chin. J. Polym. Sci.* **1999**, *17*, 551.
12. Mitra, T.; Sailakshmi, G.; Gnanamani, A.; Mandal, A. B. *J. Appl. Polym. Sci.* **2012**, *125*, E490.
13. Xiong, Y.; Wang, H.; Wu, C.; Wang, R. *Polym. Adv. Technol.* **2012**, *23*, 1429.
14. Lunstroot, K.; Driesen, K.; Nockemann, P.; Lydie, V.; Hubert Mutin, P.; Viouxb, A.; Binnemans, K. *Phys. Chem. Chem. Phys.* **2010**, *12*, 1879.
15. Tosoni1, M.; Schulz., M.; Hanemann, T. *Int. J. Electrochem. Sci.* **2014**, *9*, 3602.
16. Anthony, E. S.; Patrick, C.; H.; MacFarlane, D. R.; Forsyth, M. *Lubricants* **2013**, *1*, 3.
17. Wang, G.; Lu, X.; Ling, Y.; Zhai, T.; Wang, H.; Tong, Y.; Li, Y. *ACS Nano* **2012**, *6*, 10296.
18. Lemmon, J. P.; Lemer, M. M. *Macromolecules* **1992**, *25*, 2907.
19. Fahmi, E. M.; Ahmad, A.; Nazeri, N. N. M.; Hamzah, H.; Razali, H.; Rahman, M. Y. A. *Int. J. Electrochem. Sci.* **2012**, *7*, 5798.
20. Yahya, M. Z. A.; Arof, A. K. *J. New Mater. Electrochem. Syst.* **2002**, *5*, 123.
21. Fonseca, C. P.; Cavalcante, F., Jr.; Amaral, F.; A.; Zani Siuza, C. A.; Neves, S. *Int. J. Electrochem. Sci.* **2007**, *2*, 52.
22. Vieira, D. F.; Avellaneda, C. O.; Pawlicka, A. *Electrochim. Acta* **2007**, *53*, 1404.
23. Reddy, M. J.; Sreekanth, T.; Subba Rao, U. V. *Solid State Ionics* **1999**, *126*, 55.
24. Subba Reddy, Ch. V.; Sharma, A. K.; Narasimha Rao, V. V. R. *J. Power Sources* **2003**, *114*, 338.
25. Tanaka, K. *Acta Mater.* **2013**, *61*, 759.
26. Conway, B. E. Electrochemical Supercapacitors: Scientific Fundamentals and Technological Applications; Kluwer Academic Publishers/Plenum Press: New York, **1999**.
27. Linden, D.; Reddy, T. Handbook of Batteries, 3rd ed.; McGraw-Hill: New York, **2002**.
28. Kötz, R.; Carlen, M. *Electrochim. Acta* **2000**, *452*, 483.
29. Khomenko, V.; Raymundo-Pinero, E.; Beguin, F. *J. Power Sources* **2008**, *177*, 643.
30. Pandey, G. P.; Kumar, Y.; Hashmi, S. A. *Solid State Ionics* **2011**, *190*, 93.
31. Barsoukov, E.; Macdonald, J. R., Eds. Impedance Spectroscopy Theory, Experiment, and Applications, 2nd ed.; Wiley: New Jersey, **2005**.